Control of ellipticity in high-order harmonic generation driven by two linearly polarized fields

B. Mahieu,[1,*] S. Stremoukhov,[2,3] D. Gauthier,[4] C. Spezzani,[4] C. Alves,[1] B. Vodungbo,[5,1] P. Zeitoun,[1] V. Malka,[1,6] G. De Ninno,[7,4] and G. Lambert[1]

[1]*LOA, ENSTA ParisTech, CNRS, Ecole polytechnique, Université Paris-Saclay, 828 Boulevard des Maréchaux, 91120 Palaiseau, France*
[2]*Faculty of Physics, Lomonosov Moscow State University, Leninskie Gory, 1, Building 2, 119991 Moscow, Russia*
[3]*National Research Centre "Kurchatov Institute," 1 Akademika Kurchatova Place, Moscow 123182, Russia*
[4]*Elettra–Sincrotrone Trieste S.C.p.A., Strada Statale14 km 163.5 in AREA Science Park, 34149 Basovizza, Italy*
[5]*Sorbonne Universités, UPMC Université Paris 06, UMR 7614, LCPMR, 75005 Paris, France and CNRS, UMR 7614, LCPMR, 75005 Paris, France*
[6]*Department of Physics and Complex Systems, Weizmann Institute of Science, Rehovot, 76100, Israel*
[7]*Laboratory of Quantum Optics, University of Nova Gorica, Vipavska Cesta 11c, 5270 Ajdovščina, Slovenia*

(Received 1 February 2018; published 25 April 2018)

We demonstrate experimentally the control of the polarization (ellipticity and polarization axis) of femtosecond high-order harmonics. The method relies on a two-color ($\omega - 2\omega$) configuration, where both ω and 2ω generating fields have linear polarizations with a variable crossing angle. We correlate our measurements with the conservation rules of energy and linear momentum accounting for harmonic generation in a two-color field. We evidence that the generation process, and especially the number of ω and 2ω photons absorbed for generating a given harmonic, strongly depends on the crossing angle. Finally, relying on a simple formalism, we derive analytical formulæ for calculating both polarization axis and ellipticity of the separate harmonics. The model corroborates our results and represents a base for future investigations.

DOI: 10.1103/PhysRevA.97.043857

I. INTRODUCTION

High-order harmonic generation (HHG) of intense laser pulses in a rare gas is a source of extreme-ultraviolet (XUV) radiation, enabling the realization of time-resolved spectroscopy for the investigation of femtosecond dynamics in matter. A way to probe the physics of interaction between the rare gas atoms and the intense laser field relies on the study of the emitted radiation under perturbation of the HHG process itself, that is, *in situ* spectroscopy [1]. Control over HHG can incidentally be performed, aiming at the enhancement of XUV light features. For this purpose, the generation geometry and the waveform of the driving field may be modified. The obtained HHG enhancement typically results in an improvement of the light pulse spectral content [2], brightness [3], spatial quality [4,5], or duration. Producing harmonics with circular polarization has also become an issue at stake [6–13], motivated mostly by the growing interest of applications wishing to probe circular dichroism and chirality in matter.

A simple possibility of waveform modification relies on adding a second driving field to the fundamental beam ω, typically its second harmonic 2ω generated inline by a doubling crystal placed between the focusing lens and the gas medium [14–16]. In this scheme, both ω and 2ω are collinear, linearly polarized with angle between their polarization axes (called crossing angle θ) of 90°. Recently, we demonstrated that such a simple configuration enables the efficient generation of elliptically polarized harmonics [6]. This breakthrough allowed carrying out x-ray magnetic circular dichroism measurements at the $M_{2,3}$ absorption edge of nickel, opening the way for the investigation of (de)magnetization dynamics of materials with unprecedented temporal and spatial resolution on a tabletop installation.

Despite the latter demonstration, the understanding of the phenomenon remained only partial, though *ab initio* numerical calculations could reproduce the harmonic polarization features [17]. Moreover, harmonic polarization could not be controlled, while it will be the key feature for producing circularly polarized attosecond pulses in the future and thus probing electron motions in materials excited by ultrafast laser pulses. In this frame, we here demonstrate experimentally the possibility of achieving substantial control over the polarization of the generated harmonics and build an analytical model accounting for our scheme.

In detail, we provide in this article experimental evidence of the important role of the crossing angle in the generation process [18,19]. We consequently control the properties of polarization of the different harmonics separately, simply by changing the crossing angle between the driving fields' linear polarizations. We show the possibility to maximize the ellipticity of each harmonic and modify their polarization axis while maintaining a significant ellipticity, still preserving the flux. Different behaviors are observed from either side of the cutoff harmonic of the 2ω field, evidencing substantial differences between parallel and orthogonal crossings. Furthermore, we correlate our results with the conservation rules of HHG in two-color fields [20,21] that allow us to describe the generation of a given harmonic simply by the number of photons (n,m) absorbed from each field. The rules imply $n\omega + m(2\omega)$ for

*benoit.mahieu@ensta.fr

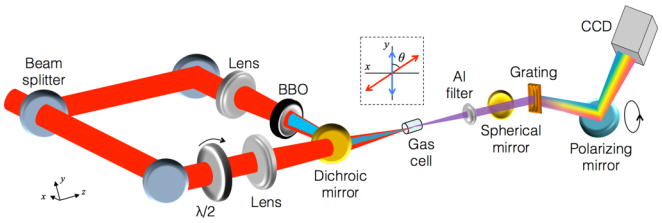

FIG. 1. The laser beam is provided by a Ti:sapphire laser source of central wavelength 810 nm, pulse duration 40 fs, and repetition rate 1 kHz. A 50:50 beam splitter sends the beam, that is originally p polarized, to two separated arms. On one arm, a half-wave plate ($\lambda/2$) allows rotating the polarization axis of ω. On the other arm, a beta barium borate (BBO) type I crystal in the *ooe* configuration generates the second harmonic of the laser with s polarization. A dichroic mirror, reflecting only the 2ω and transmitting the ω, recombines the two arms. Lenses present on the two arms tightly focus the beam into a 8-mm-long gas cell filled with argon, thus allowing the generation of the harmonic beam. The intensities of the ω and 2ω fields at focus are estimated to be $\sim 1 \times 10^{14}$ W/cm^2. A 300-nm-thick aluminium filter then cancels the ω and 2ω beams while the harmonics are characterized by means of a spectrally resolved polarization analyzer whose description can be found in Ref. [6]. It is composed of a spherical mirror at grazing incidence, a transmission grating (1000 grooves/mm), a flat polarizing mirror (SiO_2 placed at 45° incidence), and a charge-coupled device (CCD), the two latter components rotating in the transverse plane for performing the polarization scan. Not drawn in Fig. 1, a delay line enables adjusting the timing between the ω and 2ω pulses, and an additional flat mirror is placed after the spherical mirror for aligning the beam on the original optical axis.

the photon energy of a given XUV harmonic and $n\vec{k}_\omega + m\vec{k}_{2\omega}$ for its linear momentum (where $n+m$ is an odd integer, thus respecting the parity rule for dipole-allowed transitions [20,22]). We finally present our analytical model, which shows that the harmonic polarization axis and ellipticity can be calculated from the knowledge of the crossing angle and the respective contributions of the $\omega - 2\omega$ driving fields.

II. EXPERIMENTAL SETUP

The experimental setup, represented in Fig. 1, relies on a Mach-Zehnder interferometer arrangement for controlling separately the ω and 2ω fields driving HHG, and especially the crossing angle θ. A zero crossing angle corresponds to both s-polarized fields, while $\theta = 90°$ means that ω has been turned to p polarization. The HHG properties are then analyzed, as a function of θ, by means of a spectrally resolved polarization analyzer [6]. It provides, for each harmonic order, the ellipticity and the angle of the major axis of the polarization ellipse with respect to the s polarization, defining the polarization axis.

III. RESULTS

A. Spectrum

Typical harmonic spectra are represented in Fig. 2. A given harmonic can be generated either by single-color contribution $n\omega$ or $m(2\omega)$ (where n and m are odd integers), or by frequency mixing $n\omega + m(2\omega)$. Substantial differences are observed depending on the crossing angle. The most obvious concerns

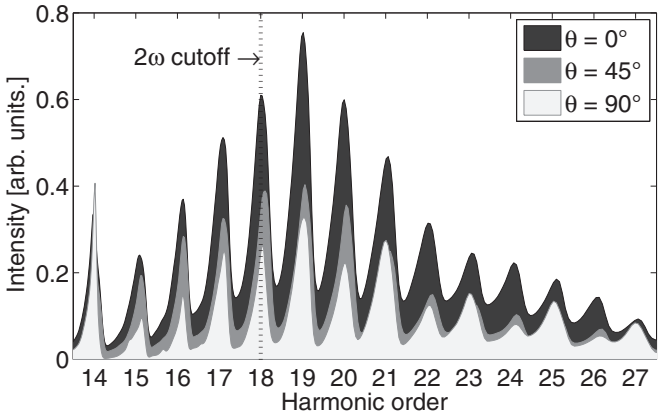

FIG. 2. Harmonic spectrum for $\theta = 0°$ (black area), $\theta = 45°$ (middle gray area), and $\theta = 90°$ (light gray area). In order to circumvent polarization dependency, the CCD signal has been averaged over a complete rotation of the polarizing mirror.

the total flux, which is 1.9 and 2.5 times larger for $\theta = 0°$ with respect to $\theta = 45°$ and $\theta = 90°$, respectively: Smaller crossing angles yield larger flux. This is in agreement with former experimental and theoretical results obtained in comparable conditions of generation [23].

More important, for $\theta = 90°$, we notice a break at the harmonic order 18. The latter is the cutoff of the spectrum when only the 2ω part drives the HHG (i.e., when the ω part is canceled). After this break, odd orders are more intense than even ones. This is because they can result either from the frequency mixing, or from the $n\omega$ contributions. For an equivalent reason, harmonic 14 is enhanced due to the strong contribution of the 2ω field in the low-energy part of the spectrum. Note that the case is different for harmonic 16, which is not an odd order of 2ω and can only result from a combination $n\omega + m(2\omega)$.

B. Polarization

For $\theta = 0°$, all harmonics are linearly polarized, but ellipticity shows up for some harmonics at relatively small crossing angles. Most of the harmonics are then elliptic when $\theta \geqslant 45°$. Figure 3(a) shows the measurements of the upper bound of ellipticity as a function of the harmonic order, for $\theta = 45°$, 75°, and 90°. We also indicated the position of harmonic 18 (2ω cutoff). For $\theta = 45°$, ellipticity is above 30% before the 2ω cutoff, after which it decreases down to 15% before increasing again toward highest orders. For $\theta \geqslant 75°$, a new regime appears: The ellipticity alternatively increases and decreases between the subsequent orders, and reaches its maxima after the 2ω cutoff. At $\theta = 75°$, this alternation is present between the harmonics 13 and 17. The ellipticity then remains above 30% after the 2ω cutoff. At higher crossing angles [see for $\theta = 90°$ in Fig. 3(a)], the odd-even alternations in terms of ellipticity are present over the whole spectrum but are reversed after the 2ω cutoff, which emphasizes the presence of this critical value. Lowest harmonics, between orders 13 and 17, have a significant but strongly varying ellipticity, from 20% to 50%. Unlike, after the 2ω cutoff, the ellipticity rises above 40% with much less variation. Interestingly, odd orders

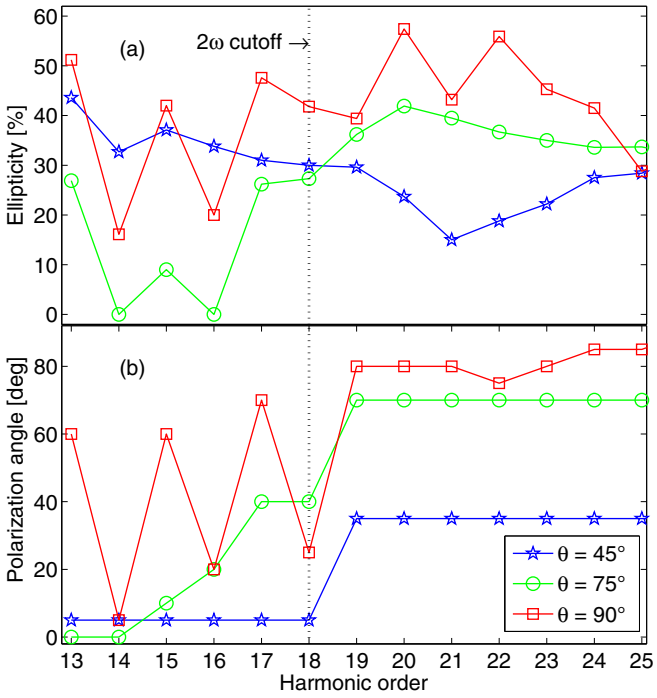

FIG. 3. (a) Measured ellipticity for $\theta = 45°$ (stars), $\theta = 75°$ (circles), and $\theta = 90°$ (squares), as a function of the harmonic order. The error is of the order of 10% for harmonics 13, 23, 24, and 25 and smaller than 5% for other orders, due to better signal-to-noise ratio. (b) Measured polarization ellipse angle with respect to the s polarization axis, for $\theta = 45°$ (stars), $\theta = 75°$ (circles), and $\theta = 90°$ (squares), as a function of the harmonic order. The error is smaller than 5° for all the harmonics.

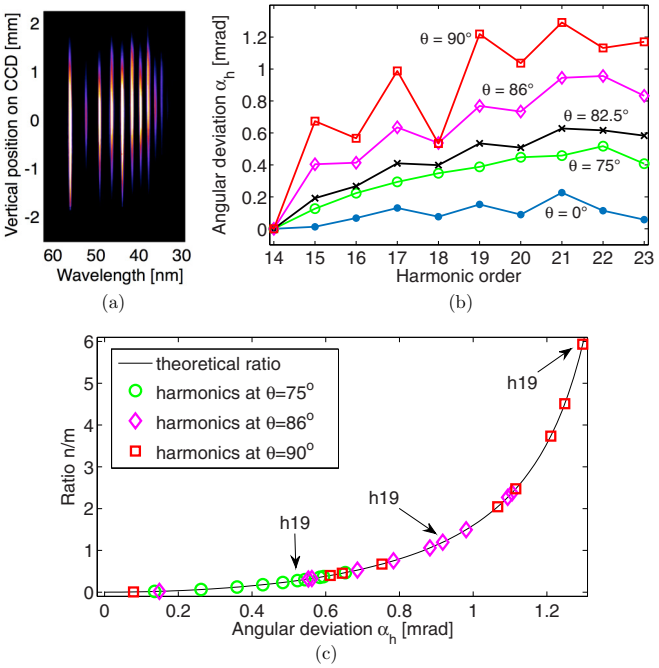

FIG. 4. (a) Raw spectrum measured for $\theta = 90°$. (b) Plot of vertical deviation of the harmonics on the spectrometer detector for $\theta = 0°$ (dots), $\theta = 75°$ (circles), $\theta = 82.5°$ (crosses), $\theta = 86°$ (diamonds), and $\theta = 90°$ (squares). The error, due to laser pointing instability, is about 0.1 mrad for all the harmonics. (c) Ratio n/m representing the relative contribution of ω and 2ω photons in the generation of an harmonic, as a function of the angular deviation of the latter. Markers correspond to the harmonics generated with $\theta = 75°$ (circles), $\theta = 86°$ (diamonds), and $\theta = 90°$ (squares). Arrows point to harmonic 19 for these three different θ.

are less elliptic than the even ones, which is attributed to the single-color contribution $n\omega$, producing a p-polarized portion of the total field. The ellipticity is maximized at even orders 20 and 22 (∼55%), which can only be produced by the mixing $n\omega + m(2\omega)$ (order 22 is beyond the 2ω cutoff).

Let us now have a look to the measured angle of the polarization ellipse, defining the polarization axis, plotted in Fig. 3(b). A threshold at the 2ω cutoff is clearly highlighted here: Whatever the crossing angle, the polarization axis of the harmonics tends to the one of the ω field (given by the crossing angle θ) for harmonics above the 18th order. Before the 2ω cutoff, there are three different behaviors. For $\theta \leqslant 45°$, the polarization axis of the harmonics is, conversely, close to the polarization axis of 2ω (corresponding an angle of 0°). For $\theta \sim 75°$, it rotates slowly toward the polarization axis of ω. For $\theta = 90°$, it is steered alternatively toward the polarization axis of ω (for odd orders, contribution of the single-color $n\omega$ part) and of 2ω (for even orders).

C. Linear momentum conservation

In order to better evaluate the respective contributions of ω and 2ω in the generation process, the ω beam was slightly tilted in the vertical direction (with respect to the propagation direction of 2ω) by an angle $\alpha_\omega = 1.5$ mrad. The induced angular deviation α_h on the harmonics was then measured. Results are reported in Figs. 4(a) and 4(b) and show an increase of the deviation with the harmonic order, following the deviation of the ω beam. The increase is more important for higher crossing angles, so that for $\theta = 90°$ and after the 2ω cutoff, the harmonics are deviated very close to the ω direction. One can notice similar trends as for ellipticity and polarization angle: an alternation between the odd-even harmonics and a peculiarity at the 2ω cutoff, the deviation for harmonic 18 decreasing significantly with respect to its neighbor harmonics. Besides, harmonic 14 always has the smallest deviation. It implies that this order is mostly the product of the $7(2\omega)$ contribution instead of a frequency mixing, which is also related to lower ellipticity and a polarization axis close to the one of 2ω (Fig. 3).

The deviation of the harmonic is directly correlated to the number (n,m) of absorbed photons. The conservation law of linear momentum $(n\vec{k}_\omega + m\vec{k}_{2\omega})$ can be easily rewritten for finding the relative contributions of ω and 2ω photons as a function of α_h:

$$\frac{n}{m} = 2\frac{\cos\alpha_h - 1}{\cos\alpha_\omega - \cos\alpha_h}, \tag{1}$$

in the case of positive values of n and m (which is justified by a $\omega/2\omega$ intensity ratio close to 1). The latter function, which tends to the ω deviation α_ω when $n \gg m$, is drawn in Fig. 4(c). On this curve, we represented the deviations measured for different values of θ [Fig. 4(b)]. It is thus clear that the higher

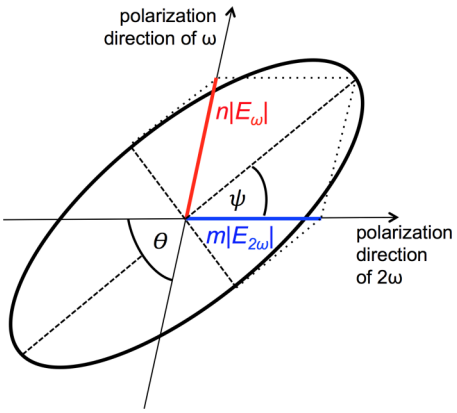

FIG. 5. Representation of the polarization ellipse of an harmonic in the $(\omega; 2\omega)$ polarization repository.

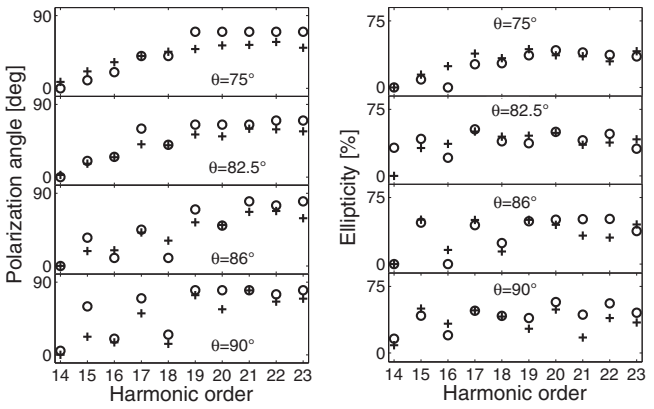

FIG. 6. Comparison between experimental measurements (circles) and the analytical model given by Eqs. (2) and (3) (crosses). Left side: polarization axis; right side: ellipticity. χ is equal to 0.2, 0.3, 0.5, and 1.5 for $\theta = 75, 82.5, 86$, and 90°, respectively.

the crossing angle, the higher the contribution of ω photons in the generation process, while for a zero crossing angle very few infrared photons are contributing ($m/n > 20$). Moreover, the ratio n/m globally increases with the harmonic order.

Different (n,m) pairs contribute to the emission of a given harmonic. The slight deviation α_ω, smaller than the harmonic divergence (∼5 mrad), does not allow us to resolve these different contributions on the detector but instead to retrieve the summed contributions. Eventually, the preferential or mean wave vector path taken for harmonic construction is easily conjectured. For example, the deviation of harmonic 19 for $\theta = 86^\circ$ is $\alpha_h = 0.92$ mrad, which corresponds to $n/m = 1.2$ [see Fig. 4(c)]. It coincides with a wave vector path almost centered on the (7,6) pair, since $7/6 \simeq 1.2$. Other pairs such as (11,4) and (3,8) are also very likely to contribute to the total emission.

IV. ANALYTICAL MODEL

Once n/m is found, we can now study quantitatively how it is correlated with the harmonic polarization. We consider the transverse projection drawn in Fig. 5, where the polarization ellipse of an harmonic is traced in a repository with axes in the directions of polarization of the two driving fields, E_ω and $E_{2\omega}$. Within this frame, pure geometrical considerations allow us to calculate both the angle of polarization axis:

$$\psi = \arcsin\left[\frac{\sin(\theta)}{\sqrt{\kappa}}\right], \tag{2}$$

and the ellipticity:

$$\epsilon = \tan\left[\frac{1}{2}\arcsin\left(\frac{2\zeta\kappa}{\zeta^2+\kappa^2}\right)\right], \tag{3}$$

with

$$\kappa = 1 + \frac{2\cos(\theta)}{\eta} + \frac{1}{\eta^2},$$

$$\zeta = \frac{\sin(\theta)}{\eta},$$

$$\eta = \chi\frac{n}{m}\frac{|E_\omega|}{|E_{2\omega}|},$$

where we introduced χ, a coupling factor between the two fields. Here we considered the common definitions of ψ and ϵ as given in Ref. [24].

To check the correctness of this model, we compare the polarization axis and ellipticity derived from the previous analytical formulas with experimental results. Figure 6 shows an excellent agreement. In particular, the odd-even alternations of ellipticity and polarization axis are well reproduced. The plateau of the polarization axis, after harmonic 18, is also predicted by the model. In the range $\theta = 0 - 90^\circ$ that we studied, the maximum theoretical ellipticity occurs for $\theta = 90^\circ$ and is 50%. It indeed corresponds to the maximal values we measured (see Fig. 3).

Equations (2) and (3) depend on four parameters. The crossing angle θ and the field ratio $|E_\omega|/|E_{2\omega}| \sim 1$ are monitored in the experiment. The photon ratio n/m is also known, as it is derived from Eq. (1). The last parameter, the coupling factor χ, was manually adjusted for optimal matching. It ranges from 0.2 for $\theta = 75^\circ$ to 1.5 for $\theta = 90^\circ$. From a classical point of view, χ can be related to the susceptibility of the medium: the higher χ, the greater the ability of the gas medium to produce circular polarization in response to the driving fields geometry.

V. CONCLUSION

In conclusion, we demonstrated the ability to control the polarization properties of femtosecond XUV pulses in a tabletop high-order harmonic source. For even simpler operation, our beamline can be easily modified to an inline implementation (i.e., without a Mach-Zehnder arrangement) by the use of band-selective wave plates.

While this possibility was not obvious [25,26] until recently [6,17], we thus confirm that it is possible to generate elliptically polarized harmonics by means of a combination of linearly polarized driving fields. Though counterintuitive, this observation is not in contradiction with the conservation of spin angular momentum (associated to the circular polarization of the light) from the linearly polarized photons of the driving field to the harmonic photons [17]. Indeed, linear polarization can be seen as the addition of two counter-rotating circular polarizations,

thus carrying spin angular momentum with opposite sign, which can eventually be transferred to the harmonics.

Our control parameter is the crossing angle between the polarizations of ω and 2ω. We studied its action on the different harmonic properties: ellipticity, spectrum, polarization axis, and relative fields' contribution (n/m ratio). By increasing the crossing angle toward 90°, alternations between odd and even orders are observed for the different properties. A break is moreover observed at the 18th order, that is, the cutoff harmonic of 2ω. For a fixed crossing angle of 90°, the average ellipticity was 40%. In addition, the ellipticity of a given harmonic can be maximized by simply changing the crossing angle between the polarizations of ω and 2ω, but never beyond 50%.

Finally, we developed a model allowing to calculate both the ellipticity and the polarization axis of the harmonics. Based on a classical nonlinear optics frame, it successfully reproduces experimental measurements and thus potentially enables us to predict and monitor the harmonics polarization features. Such model is moreover a requisite for fine understanding of the generation process accounting for present and eventually further complex configurations.

The present study shall be extended toward higher crossing angles accompanied by the control of the ω-2ω relative phase. It would allow us to determine the possibility of generating fully circular harmonics in this configuration and of controlling the helicity of subsequent harmonics, and thus of potentially generating attosecond pulses with circular polarization [27].

ACKNOWLEDGMENTS

This work has been achieved through the Laserlab-Europe consortium, with the financial support of the X-Five Grant No. 339128 from the European Reasearch Council and the UMAMI grant from the French National Research Agency. The authors warmly thank P. Salières for fruitful discussions and M. Lozano for the laser supply.

[1] N. Dudovich, O. Smirnova, J. Levesque, Y. Mairesse, M. Yu. Ivanov, D. M. Villeneuve, and P. B. Corkum, Measuring and controlling the birth of attosecond xuv pulses, Nat. Phys. **2**, 781 (2006).

[2] B. Mahieu, S. Coraggia, C. Callegari, M. Coreno, G. De Ninno, M. Devetta, F. Frassetto, D. Garzella, M. Negro, C. Spezzani *et al.*, Full tunability of laser femtosecond high-order harmonics in the ultraviolet spectral range, Appl. Phys. B **108**, 43 (2012).

[3] L. E. Chipperfield, J. S. Robinson, J. W. G. Tisch, and J. P. Marangos, Ideal Waveform to Generate the Maximum Possible Electron Recollision Energy for Any Given Oscillation Period, Phys. Rev. Lett. **102**, 063003 (2009).

[4] J. Gautier, P. Zeitoun, C. Hauri, A.-S. Morlens, G. Rey, C. Valentin, E. Papalarazou, J.-P. Goddet, S. Sebban, F. Burgy *et al.*, Optimization of the wave front of high order harmonics, Eur. Phys. J. D **48**, 459 (2008).

[5] B. Mahieu, D. Gauthier, M. Perdrix, X. Ge, W. Boutu, F. Lepetit, F. Wang, B. Carré, T. Auguste, H. Merdji, D. Garzella, and O. Gobert, Spatial quality improvement of a Ti:sapphire laser beam by modal filtering, Appl. Phys. B **118**, 47 (2015).

[6] G. Lambert, B. Vodungbo, J. Gautier, B. Mahieu, V. Malka, S. Sebban, P. Zeitoun, J. Luning, J. Perron, A. Andreev *et al.*, Towards enabling femtosecond helicity-dependent spectroscopy with high-harmonic sources, Nat. Commun. **6**, 6167 (2015).

[7] A. Ferré, C. Handschin, M. Dumergue, F. Burgy, A. Comby, D. Descamps, B. Fabre, G. A. Garcia, R. Géneaux, L. Merceron *et al.*, A table-top ultrashort light source in the extreme ultraviolet for circular dichroism experiments, Nat. Photon. **9**, 93 (2015).

[8] A. Fleischer, O. Kfir, T. Diskin, P. Sidorenko, and O. Cohen, Spin angular momentum and tunable polarization in high-harmonic generation, Nat. Photon. **8**, 543 (2014).

[9] D. D. Hickstein, F. J. Dollar, P. Grychtol, J. L. Ellis, R. Knut, C. Hernández-García, D. Zusin, C. Gentry, J. M. Shaw, T. Fan *et al.*, Non-collinear generation of angularly isolated circularly polarized high harmonics, Nat. Photon. **9**, 743 (2015).

[10] J. Levesque, Y. Mairesse, N. Dudovich, H. Pépin, J.-C. Kieffer, P. B. Corkum, and D. M. Villeneuve, Polarization State of High-Order Harmonic Emission from Aligned Molecules, Phys. Rev. Lett. **99**, 243001 (2007).

[11] B. Vodungbo, A. B. Sardinha, J. Gautier, G. Lambert, C. Valentin, M. Lozano, G. Iaquaniello, F. Delmotte, S. Sebban, J. Lüning, and P. Zeitoun, Polarization control of high order harmonics in the EUV photon energy range, Opt. Express **19**, 4346 (2011).

[12] A. Depresseux, E. Oliva, J. Gautier, F. Tissandier, G. Lambert, B. Vodungbo, J.-P. Goddet, A. Tafzi, J. Nejdl, M. Kozlova *et al.*, Demonstration of a Circularly Polarized Plasma-Based Soft-x-ray Laser, Phys. Rev. Lett. **115**, 083901 (2015).

[13] O. Kfir, E. Bordo, G. I. Haham, O. Lahav, A. Fleischer, and O. Cohen, In-line production of a bi-circular field for generation of helically polarized high-order harmonics, Appl. Phys. Lett. **108**, 211106 (2016).

[14] G. Lambert, A. Andreev, J. Gautier, L. Giannessi, V. Malka, A. Petralia, S. Sebban, S. Stremoukhov, F. Tissandier, B. Vodungbo, and P. Zeitoun, Spatial properties of odd and even low order harmonics generated in gas, Sci. Rep. **5**, 7786 (2015).

[15] G. Lambert, F. Tissandier, J. Gautier, C. P. Hauri, P. Zeitoun, C. Valentin, T. Marchenko, J.-P. Goddet, M. Ribière, A. B. Sardinha *et al.*, Aberration-free high-harmonic source generated with a two-colour field, Europhys. Lett. **89**, 24001 (2010).

[16] G. Lambert, J. Gautier, C. P. Hauri, P. Zeitoun, C. Valentin, T. Marchenko, F. Tissandier, J.-P. Goddet, M. Ribière, G. Rey *et al.*, An optimized KHz two-colour high harmonic source for seeding free-electron lasers and plasma-based soft x-ray lasers, New J. Phys. **11**, 083033 (2009).

[17] S. Stremoukhov, A. V. Andreev, B. Vodungbo, P. Salières, B. Mahieu, and G. Lambert, Origin of ellipticity of high-order harmonics generated by a two-color laser field in the cross-polarized configuration, Phys. Rev. A **94**, 013855 (2016).

[18] A. V. Andreev, S. Stremoukhov, and O. A. Shoutova, High-order optical harmonic generation in ionization-free regime: Origin of the process, J. Opt. Soc. Am. B **30**, 1794 (2015).

[19] A. V. Andreev, S. Stremoukhov, and O. A. Shoutova, Light-induced anisotropy of atomic response: Prospects for emission spectrum control, Eur. Phys. J. D **66**, 16 (2012).

[20] M. D. Perry and J. K. Crane, High-order harmonic emission from mixed fields, Phys. Rev. A **48**, R4051 (1993).

[21] J. B. Bertrand, H. J. Wörner, H.-C. Bandulet, E. Bisson, M. Spanner, J.-C. Kieffer, D. M. Villeneuve, and P. B. Corkum, Ultrahigh-Order Wave Mixing in Noncollinear High Harmonic Generation, Phys. Rev. Lett. **106**, 023001 (2011).

[22] A. Fleischer and N. Moiseyev, Attosecond laser pulse synthesis using bichromatic high-order harmonic generation, Phys. Rev. A **74**, 053806 (2006).

[23] H. Eichmann, A. Egbert, S. Nolte, C. Momma, B. Wellegehausen, W. Becker, S. Long, and J. K. McIver, Polarization-dependent high-order two-color mixing, Phys. Rev. A **51**, R3414(R) (1995).

[24] P. Antoine, A. L'Huillier, M. Lewenstein, P. Salières, and B. Carré, Theory of high-order harmonic generation by an elliptically polarized laser field, Phys. Rev. A **53**, 1725 (1996).

[25] C. Ruiz, D. J. Hoffmann, R. Torres, L. E. Chipperfield, and J. P. Marangos, Control of the polarization of attosecond pulses using a two-color field, New J. Phys. **11**, 113045 (2009).

[26] D. Shafir, Y. Mairesse, H. J. Worner, K. Rupnik, D. M. Villeneuve, P. B. Corkum, and N. Dudovich, Probing the symmetry of atomic wave functions from the point of view of strong field-driven electrons, New J. Phys. **12**, 073032 (2010).

[27] L. Medišauskas, J. Wragg, H. van der Hart, and M. Y. Ivanov, Generating Isolated Elliptically Polarized Attosecond Pulses Using Bichromatic Counterrotating Circularly Polarized Laser Fields, Phys. Rev. Lett. **115**, 153001 (2015).